MEMOIRS OF THE FACULTY OF ENGINEERING
FUKUI UNIVERSITY
VOL.26 No.2 1978

LOW TEMPERATURE NMR APPARATUS WITH MOSFETS (3SK45) AND $Al_2O_3:Al^{27}$ NMR EXPERIMENTS

Hisao YAGI, Masasi INOUE, Toshiaki TATSUKAWA* and Kenji KURIMOTO

(Received May 31, 1978)

Thermal hysteresis tests have been made between 300 and 77 K for the static characteristics of commercial MOSFETs (3SK45) which are to be used as active elements in our steady-state NMR apparatus. The newly constructed apparatus using this type of FETs works well at low temperatures, with respect to the reproducibility, stability, and signal-to-noise ratio. With this device, the Al^{27} NMR in ruby crystal ($Al_2O_3:Cr^{3+}$) has been measured at 77 K and liquid helium temperatures. Both the dipolar splitting width and the absorption intensity in the NMR spectrum depend on temperature and the angle between the magnetic field and the trigonal axis. These results are explained by the spin diffusion model, in which the Al^{27} nuclei see the local fields arising from identical nucear spins and the paramagnetic electron spins of Cr^{3+} ions existing in the crystal.

1. INTRODUCTION

In the past several years we have been trying to improve a low temperature steady-state NMR apparatus using commercial MOSFETs as active elements; thus far dual-gate n-channel type FETs (Toshiba: 3SK35-5J) have been used. In order to study the reproducibility of these FET elements, we have previously carried out several heat cycle tests, in which are measured the variations of the static characteristics of the elements after repeated cooling and warming between 300 and 77 K.[1] As a result, some FETs have a good reproducibility and some do not.

In the present work, we have examined the similar thermal hyster-

Dept. of Applied Physics.
* Experimental Laboratory for Low Temperature Physics.

esis of another commercial FETs (Hitachi: 3SK45-6B3)* and constructed the marginal type steady-state NMR apparatus with these elements including the oscillator and amplifier. With this new apparatus we have again performed the NMR measurements of Al^{27} nuclei in ruby crystal (Al_2O_3: Cr^{3+}) at liquid helium temperatures and compared the results with previous data[2] obtained by the early apparatus with 3SK35-5J. Discussions about the observed NMR signals in terms of a spin diffusion model are presented, in particular their temperature and angular dependences.

2. HEAT CYCLE TEST

The variations of the static characteristics of dual-gate MOSFETs (3SK45-6B3) after repeated heat cycles were measured by the test circuit used previously,[1] where the heat cycle (h.c.) means the repeated cooling and warming of the FETs between 300 and 77 K. At both termperatures, the drain-source current I_{DS} was measured as a function of the gate 1-source voltage V_{G1S} at two fixed gate 2-source voltages V_{G2S} (=0 or 2 V), the drain-source voltage V_{DS} being kept at a constant value (=12 V). This procedure is the same as the previous experiments. Typical results for a FET with good reproducibilty and that with poor one are shown in Fig. 1.

It is seen that the I_{DS}-V_{G1S} characteristics of a good FET are fairly reproducible and the variations are smooth; the cut-off voltage shifts from -1 V at 300 K to -0.5 V at 77 K. In the case of a bad FET, the static characteristics have poor reproducibility and the variations are rather irregular; the cut-off voltage at 77 K varies considerably. Though not decisive, from a comparison between the two types of commercial FETs (3SK45-6B3 and 3SK35-5J) we found that the former seems to have a high percentage of good reproducibility (say, the number of good FETs out of ten FETs) compared with the latter. We are not sure whether the difference is due to a fabrication method of the FETs. In either case, however, when these FETs are used as active elements in our NMR apparatus, the most probable bias voltages are to be recommended as follows; V_{G1S}= -1 $\sim$ 0.5 V for an oscillator, V_{G1S}=0 for a class A amplifier, V_{G2S}=1 V for all circuits, and V_{DS}=3 $\sim$ 4 V.

---

* We are grateful to Dr. A. Nakamura (Electrotechnical Laboratory, Tanashi, Tokyo) for calling our attention to this type of FETs.

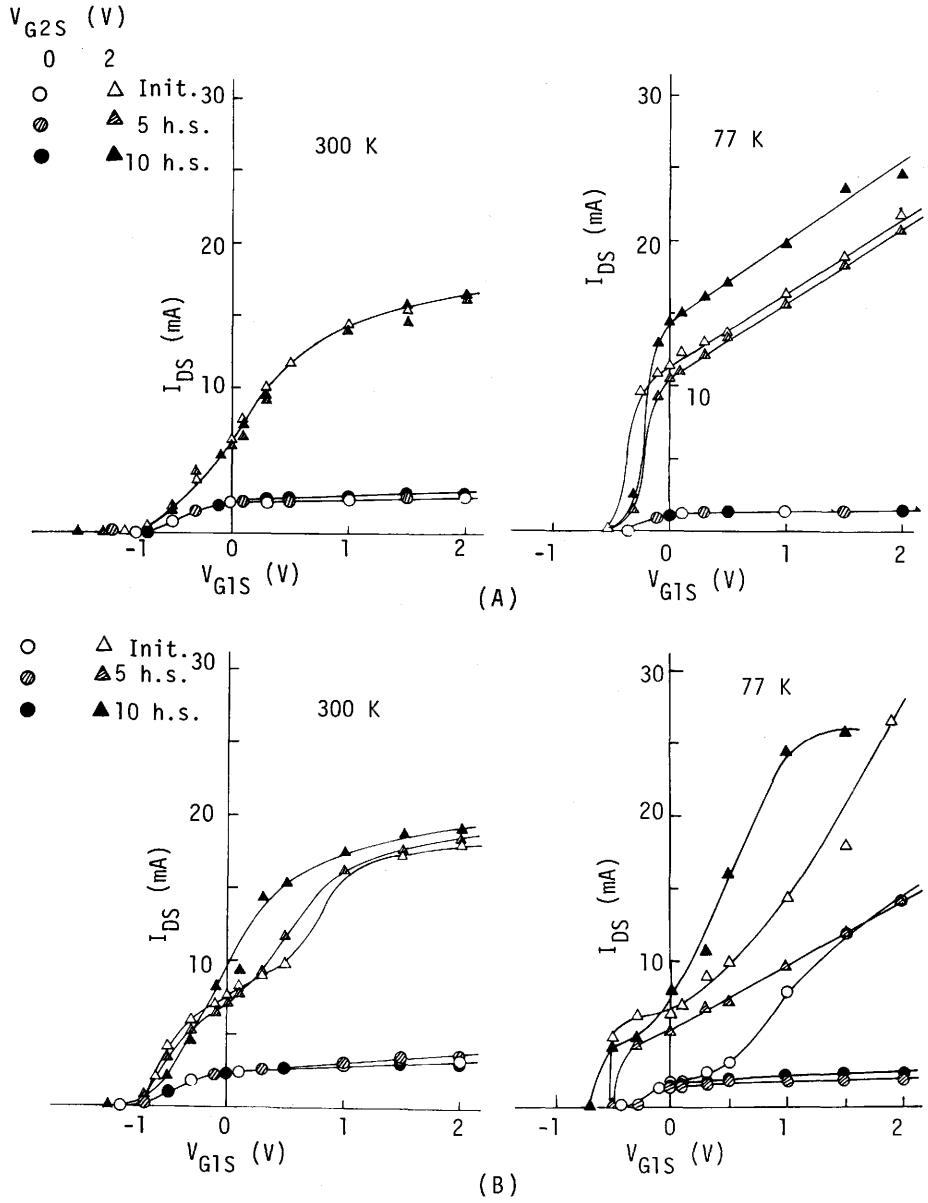

Fig. 1. The I_{DS}-V_{G1S} characteristics at 300 and 77 K of the dual-gate MOSFET (3SK45-6B3) at the initial state (as-purchased) and after repeated heat cycles (5 and 10 times), measured at two different gate 2-source voltages V_{G2S}= 0 or 2 V.
(A):a FET with good reproducibility. (B):a FET with poor reproducibility.

3. NMR APPARATUS

By taking account of these various factors and together with some modifications of the previous circuits,[3,4] we have constructed a new NMR apparatus, as shown in Fig. 2. Once use was made of a FET element instead of a crystal diode in the detector circuit so that the whole circuits (oscillator, amplifier, and detector) could be imbedded in a cryogenic capsule,[4] but the result was not good enough to get a stable operation. Then we again cited the original method of the diode detection, but with an additional low-pass filter. A brief description of the working principle is given below.

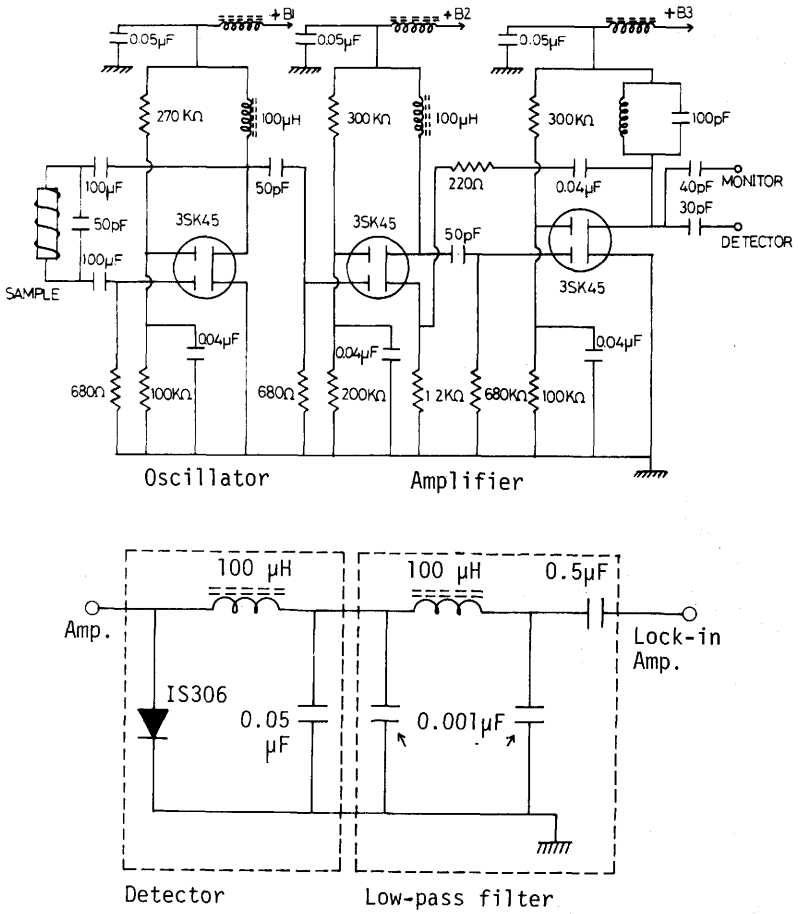

Fig. 2. Newly constructed NMR apparatus using dual-gate type MOSFETs (3SK45-6B3) as active elements.

A high frequency oscillation takes place at the oscillator circuit consisting of a sample coil (tank circuit) and a FET. The output from the drain terminal is fed to the first-stage amplifier followed by the second-stage one, both of class A, where another tuning circuit is installed at the output (drain) terminal to ensure a frequency stabilization. Part of the output signal is fed back to the source terminal of the first-stage amplifier for the stabilization of the amplifiers. The other output is transmitted to the detector circuit and then to a lock-in amplifier. To improve an S/N ratio, high frequency blocking coils are installed to each +B supply. Except the detector circuit which should be kept at room temperature, the whole part are assembled on a printed bakelite base, 2 cm x 20 cm, which is then encapsulated in a copper tubing for a low temperature NMR measurements.

Prior to the NMR experiments, we examined an oscillation characteristic of the constructed apparatus. The results obtained at 300, 77, and 4.2 K are shown in Fig. 3, where the oscillation voltages V_{osc} measured by an oscilloscope at the monitor terminal are plotted against the $+B_1$ voltage (or V_{DS} voltage of the FET), both $+B_2$ and $+B_3$ voltages of the amplifiers being kept constant (= 4V). The observed curves are characteristic of a marginal type oscillation. The oscillation stops at different $+B_1$ voltages for these three temperatures,

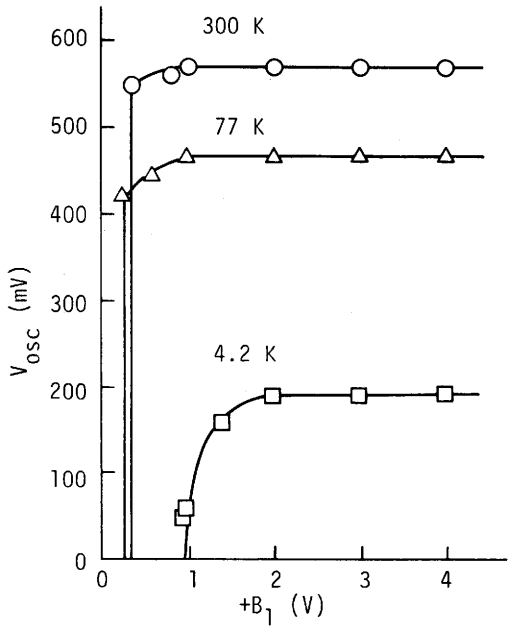

Fig. 3. Oscillation characteristics at three different temperatures.

which may be due to the variation of the I_{DS}-V_{G1S} characteristics of the FET with temperature. For NMR experiments, the $+B_1$ voltage was set just before the oscillation stop.

4. STEADY-STATE NMR EXPERIMENT

4.1. Magnetic field modulation

The NMR measurements of Al^{27} in ruby crystal (Al_2O_3:Cr^{3+}) were made by a conventional magnetic field modulation technique. As is well known, both the modulation amplitude H_m and the frequency f_m have an effect on a resonance line (Gaussian or Lorentzian). Generally, a maximum absorption signal is attained at the condition of $H_m=2\Delta H_{pp}$ for a Gaussian line and $H_m=3\ \Delta H_{pp}$ for a Lorentzian line, where ΔH_{pp} is the true peak-to-peak linewidth. The observed linewidth differs from the true linewidth and depends on the amplitude. Thus it is desirable to set the modulation amplitude to at least half the actual linewidth; in the case of Al^{27} NMR H_m should be less than 0.5 G. However, for a small modulation amplitude the observed intensity or S/N ratio decreased markedly. Because of our experimental limitations, the measurements were carried out under the modulation amplitude ranging from 10 to 40 G.

On the other hand, the modulation frequency $\omega_m=2\pi f_m$ must ordinarily satisfy the condition as

$$\omega_m < \gamma\Delta H_{pp} \text{ with } \gamma=g\beta/\hbar, \text{ or roughly } f_m < 1/T_1,\ 1/T_2, \quad (1)$$

where T_1 and T_2 are the spin-lattice and spin-spin relaxation times, respectively. The measurements by Verber et al.[5] show that the spin-lattice relaxation time of Al^{27} nuclei in ruby crystal is of the order of $0.1 \sim 1$ sec at 4.2 K; thus f_m must be within the range of $1 \sim 10$ Hz. One example of the effect of the modulation frequency on the Al^{27} absorption intensity at 77 and 4.2 K is shown in Fig. 4, where the absorption intensity of the $m=1/2 \leftrightarrow -1/2$ line is plotted against the modulation frequency with the amplitude H_m indicated. These results are in agreement with previous data[6] which were taken by the early apparatus with MOSFETs (3SK35-5J). The maximum intensity is located around $f_m \simeq 10$ Hz at 77 K and approximately 1 Hz at 4.2 K, in reasonable agreement with the corresponding spin-lattice relaxation times found by Verber et al.

4.2. Signal-to-noise ratio

Furthermore, it is known that a scanning rate, at which the applied magnetic field is scanned, is also responsible for the detected

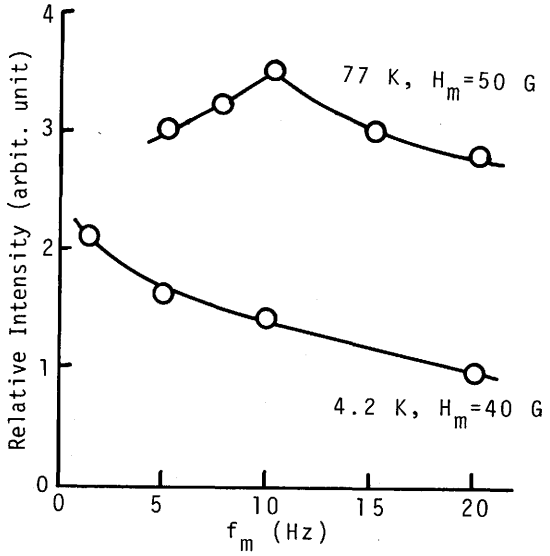

Fig. 4. Relative absorption intensity of the Al^{27} NMR line, corresponding to m=1/2 ↔ -1/2 transition, as a function of modulation frequency with different amplitudes, measured at 77 and 4.2 K.

signals. In the present experiment the scanning rate dH/dt was set constant at 80 G/min. Under these conditions described hitherto, the NMR measurements were carried out at low temperatures using a home-made metal dewar. The angle θ between the magnetic field and the trigonal (c-) axis of the ruby crystal was varied by rotating an electromagnet.

At first, in Fig. 5 are illustrated the typical five-line spectra at different temperatures. The experimental conditions are given in the caption such as the static magnetic field H_o, oscillation frequency f_o, modulation amplitude H_m and its frequency f_m. It is evident that the S/N ratio increases with decreasing temperature. Moreover, we have compared the differences in the S/N ratios observed only by replacing the one type of FET elements by the other type (3SK45 and 3SK35) in the circuits. Such a replacement can be made because the working conditions or the static characteristics of both FETs are almost equal to each other. The results taken at 77 and 4.2 K are given in Table I, other experimental conditions being kept constant. At 77 K there seems to be no difference between the two

FET	77 K	4.2 K
3SK35-5J	5	12
3SK45-6B3	6	40

Table I. S/N ratios of Al^{27} NMR signals at 77 and 4.2 K, measured by the same apparatus but with different MOSFETs.

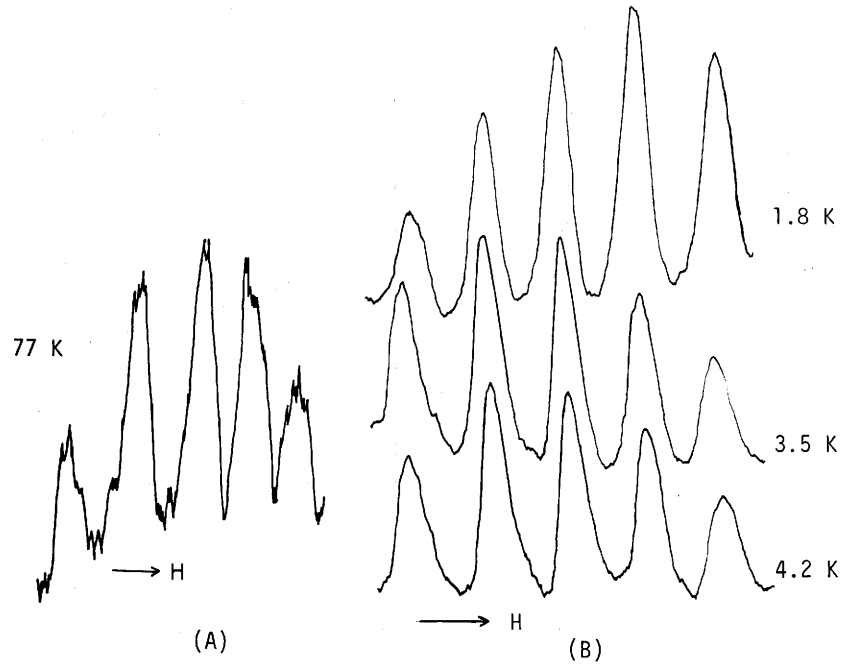

Fig. 5. The observed NMR signals of Al^{27} in ruby crystal ($\theta=0°$) at different temperatures, taken by the present apparatus using MOSFETs 3SK45-6B3.
(A):H_o=17.42 kG, f_o=19.339 MHz, H_m=40 G, and f_m=10 Hz.
(B):H_o=17.70 kG, f_o=19.658 MHz, H_m=40 G, and f_m=10 Hz.

FETs, while at 4.2 K the apparatus with 3SK45-6B3 has a higher S/N ratio than that with 3SK35-5J.

4.3. Absorption spectrum

The five nuclear magnetic resonance lines in the ruby crystal are known to have a partially resolved structure for each of the five lines, which is ascribed to nuclear dipole-dipole interaction.[7] However, this structure could not be resolved by our previous apparatus. Now the improved apparatus enables us to observe the expected structure. Figure 6 shows the resolved spectrum for $\theta=0°$ at 4.2 K. The observed splitting width is large compared with the reported value ($\Delta H=10 \sim 20$ G at 4.2 K).[5] The shape of these spectra varies with rotating the magnetic field direction with respect to the c-axis of crystal. The original splitting of the spectrum is due to the electric quadrupole interaction and the satellite lines arise from the dipole-dipole coupling.

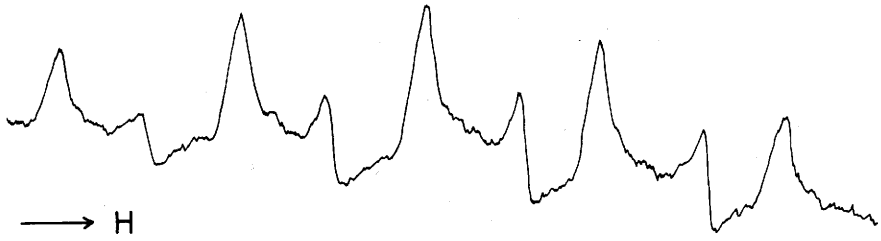

Fig. 6. The partially resolved Al^{27} NMR spectrum for $\theta=0°$ at 4.2 K; $H_o=17.92$ kG, $f_o=19.713$ MHz, $H_m=40$ G, and $f_m=10$ Hz.

The main absorption spectrum can be explained by the following Hamiltonian for a nuclear spin in the presence of a magnetic field and an electric field gradient,

$$H_o=\gamma\hbar H_o I_z + \frac{eqQ}{4I(2I-1)}(3I_z^2 - I^2), \tag{2}$$

where γ is the nuclear magnetogyric ratio and eqQ is the quadrupole coupling constant. In addition, the dipole-dipole coupling is effective and its magnitude is written by

$$d = (\gamma/2\pi)^2 hr^{-3}\frac{1}{2}(3\cos^2\theta - 1), \tag{3}$$

where r is the internuclear distance and θ is the angle between the c-axis and the magnetic field. Then, the Hamiltonian for two identical spins in a magnetic field with the same quadrupole interaction and direct dipole-dipole interaction is expressed as

$$H = \gamma\hbar H_o(I_{1z} + I_{2z}) + \frac{eqQ}{4I(2I-1)}(3I_{1z}^2 + 3I_{2z}^2 - I_1^2 - I_2^2)$$

$$+ d(I_1\cdot I_2 - 3I_{1z}I_{2z}). \tag{4}$$

In Fig. 7 are illustrated (A) the schematic line shape, (B) the angular dependence of the dipolar splitting width at 4.2 K corresponding to each main transition, and (C) the temperature dependence of the width at $\theta=0°$. The absorption spectrum drawn schematically in Fig. 7(A) is based upon the above Hamiltonian. The dipolar splitting becomes the maximum when =0° and it is expected to vanish at $3\cos^2\theta$ =1 ($\theta\simeq 54°$). Some points lack in Fig. 7(B) because of experimental uncertainty.

The temperature dependence of the dipole-dipole coupling constant is expected to be negligible, when it is due to the identical nuclear

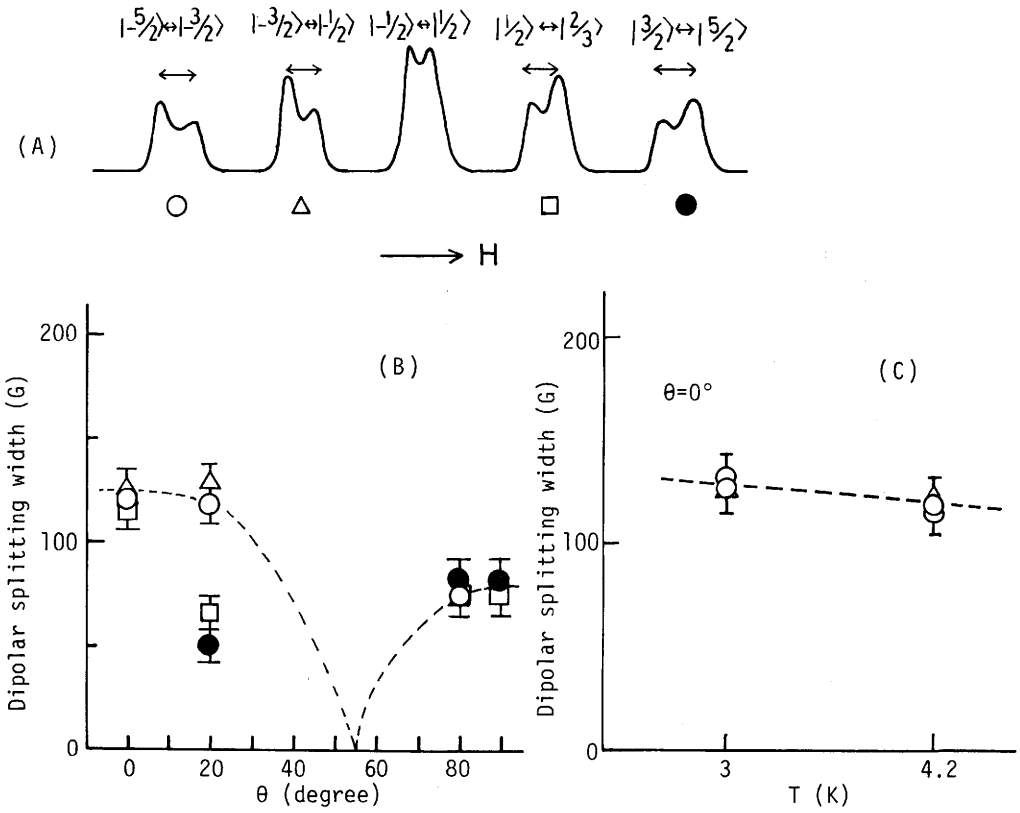

Fig. 7. (A) A schematic absorption spectrum of Al^{27} NMR in ruby. (B) The angular dependence of the dipole-dipole splitting width at 4.2 K, the indicated symbols corresponding to each main transition shown in (A). The dotted curve shows a variation of the form $(3\cos^2\theta - 1)$. (C) The dipolar splitting width at $\theta=0°$ vs temperature.

spins, as given in eq.(3). However, the experimental results shown in Fig. 7 (C) are the contrary; an increase in the splitting width with decreasing temperature. This suggests that in addition to the mutual interaction of the Al^{27} spins, the paramagnetic spins of Cr^{3+} ions will contribute to the splitting width; that is, the existence of dipole-dipole coupling between electron spins and nuclear spins. The nuclear spins see the local fields arising from the electron spins, whose strength will vary with temperature, since the effective magnetic moments of the Cr^{3+} ions are the Boltzman average of the moments due to its electron spin states which are splitted by crystalline field.

4.4. Angular dependence of the absorption intensity

In addition to the dipolar splitting width, we have paid attention to the intensity of the absorption spectrum. Figure 8 demonstrates the angular variation of the m=-1/2 ↔ 1/2 transition line, for which the magnetic resonance field H_o does not shift with the angle within the first order perturbation of the quadrupole interaction. The measurements were carried out at 4.2 K under the experimental conditions indicated, with the modulation amplitude (A) H_m=40 G and (B) H_m =10 G. The angular dependences of the absorption intensities mea-

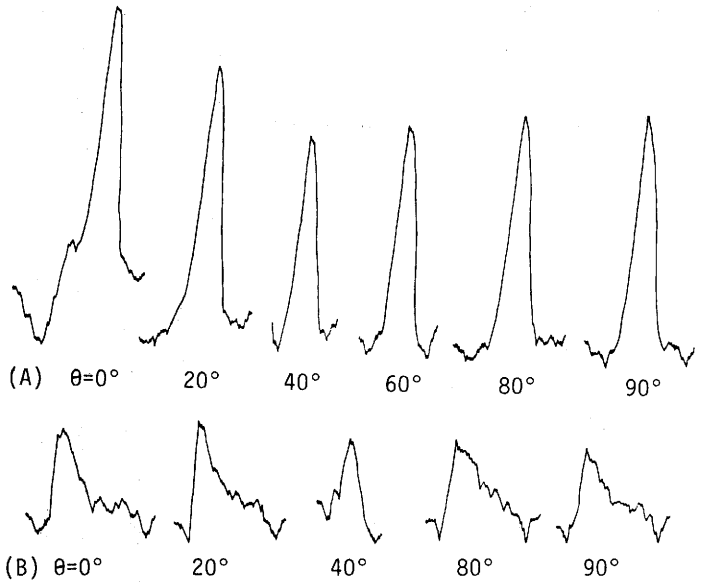

Fig. 8. The variation of the m=-1/2 ↔ 1/2 transition line with the angle at 4.2 K, measured under the same experimental conditions except H_m; H_o=17.92 kG, f_o=19.713 MHz, and f_m=10 Hz. (A) H_m=40 G; (B) H_m=10 G.

sured at different conditions are shown in Figs. 9(A), (B), and (C), where the parameters are the modulation amplitude H_m, modulation frequency f_m, and temperature T, respectively.

Figure 9(A) shows that the relative intensity increases with the modulation amplitude, as expected. In the case of a Gaussian shape, the manimum intensity attains at the condition $H_m=2\Delta H_{pp}$, which approximately corresponds to the experimental result of the observed peak-to-peak width $\Delta H_{pp}\simeq$15 G at 4.2 K. The experimental points lie on a theoretically predicted curve as $(1 - 3\cos^2\theta)^2$.

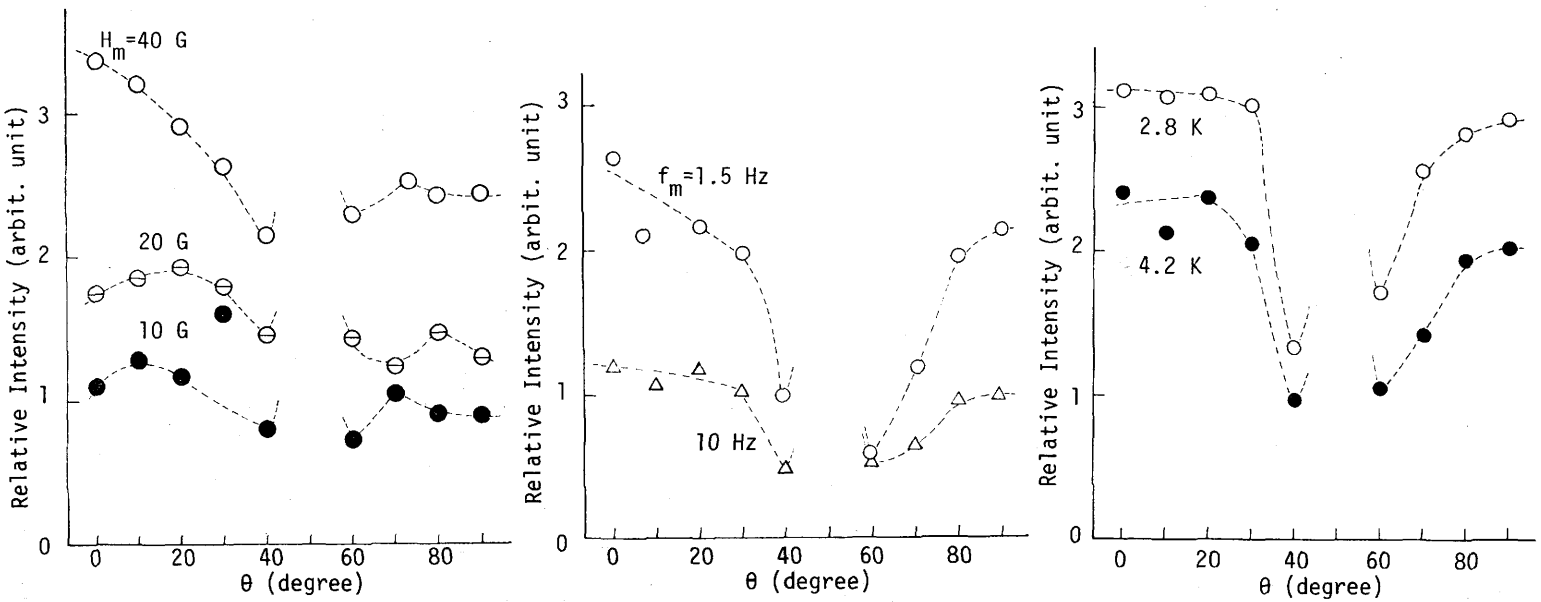

(A) T=4.2 K, f_m=10 Hz (B) T=4.2 K, H_m=40 G (C) H_m=40 G, f_m=10 Hz

Fig. 9. Angular dependences of the relative intensity of the m=-1/2 ↔ 1/2 transition line measured under the different conditions indicated, the resonance condition H_o=17.92 kG and f_o=19.713 MHz being kept constant.

Figure 9(B) indicates that the relative intensity at 4.2 K becomes larger at lower modulation frequency, in good agreement with the results shown in Fig. 4; there we noted a correlation between the modulation frequency and the spin-lattice (or spin-spin) relaxation time.

Finally, from Fig. 9(C) the intensity is seen to increase as the temperature is decreased; this behavior is consistent with the result shown in Fig. 7(C) that the paramagnetic Cr^{3+} ions (electron spins) contribute to the nuclear spin resonance.

In all these curves there lack the points between $\theta=40°$ and 60°, because all the absorption lines due to the quadrupole splitting converge at $\sim 54°$ to a large single line.

5. CONCLUSION

In the preceding sections, we have noted that the dipolar splitting width [Fig. 7(C)] and the relative absorption intensity (Fig. 9) of the Al^{27} NMR spectrum in ruby crystal depend upon temperature. This is also the case for the linewidth measured previously.[2] These phenomena are attributed to the presence of paramagnetic Cr^{3+} ions in the crystal. From the past the basic understanding has been given of the problem of the spin relaxation of nuclei in a crystal containing paramagnetic impurities when the transfer of spin energy to the lattice is limited by the diffusion of nuclear energy.[5,8,9] Our results obtained by the NMR apparatus using MOSFETs can be qualitatively explained by the concept of such a spin diffusion model.

ACKNOWLEDGMENTS

Thanks are due to S. Nishizawa and H. Ikehata for their help in the present experiment and K. Tsubokawa and T. Saito for cryogenic and technical assistance.

REFERENCES

1) H. Yagi, M. Inoue, T. Tatsukawa and K. Kurimoto: Memoirs Fac. Eng. Fukui Univ. 25 (1977) 55.
2) M. Takeuchi, T. Tatsukawa, M. Inoue and H. Yagi: Memoirs Fac. Eng. Fukui Univ. 23 (1975) 271 [in Japanese].
3) H. Yagi, M. Inoue, T. Tatsukawa, T. Naito and M. Takeuchi: Cryogenic Engineering 11 (1976) 18 [in Japanese].
4) T. Tatsukawa, M. Nakamura, M. Inoue and H. Yagi: Memoirs Fac. Eng. Fukui Univ. 24 (1976) 319 [in Japanese].
5) C. M. Verber, H. P. Mahon and W. H. Tanttila: Phys. Rev. 125 (1962) 1149.
6) M. Takeuchi: M.A. Thesis, Fukui Univ., 1976 (unpublished).
7) A. H. Silver, T. Kushida and J. Lambe: Phys. Rev. 125 (1962) 1147.
8) N. Bloembergen: Physica 25 (1949) 386.
9) W. E. Blumberg: Phys. Rev. 119 (1960) 79.